

# Computational Efficient Model for Human Ventricular Epicardial Cells

Niccoló Biasi<sup>1</sup>, Alessandro Tognetti<sup>1,2</sup>

<sup>1</sup> Dipartimento di Ingegneria dell'Informazione, Università di Pisa, Italy

<sup>2</sup> Centro E. Piaggio, Università di Pisa, Italy

## Abstract

*We developed a new phenomenological model for ventricular epicardial cells. The proposed model is based on the Rogers-McCulloch formulation of the FitzHugh-Nagumo equations and consists of only three state variables. Furthermore, our model includes a simplification parameter  $r_\gamma$  which allows increasing time and space integration by a factor equal to  $r_\gamma$ . Our three-variable model can reproduce the main tissue-level characteristics of epicardial cells, such as action potential amplitudes and shapes, upstroke velocities, and action potential duration and conduction velocity restitution curves. Except for a reduced upstroke velocity, the simplification included in the model does not significantly affect action potential characteristics and restitution properties. In a 2D sheet, integral characteristics of reentry dynamics, such as dominant period, are only slightly influenced by the simplification. However, the trajectory of the spiral tip changes for different values of  $r_\gamma$ .*

## 1. Introduction

Mathematical models of the electrical activity of the heart are recognized as useful tools for understanding cardiac functions and diseases. Mathematical simulations are widely used in the literature to study reentrant phenomena in the human cardiac tissue (e.g. [1–3]). Modelling wave propagation in human ventricular tissue requires the use of ionic models specific for human ventricular cells. Cardiac ionic models should reproduce accurately all the key characteristics of action potential (AP) propagation to correctly simulate dynamics of reentrant waves. Moreover, it is desirable to maintain as low as possible the computational complexity of the model to facilitate large-scale 3D simulations, especially when using highly detailed anatomical structures. In addition, a lower number of model parameters make easier the process of fitting the model to experimental data. Ionic models can be divided in two categories: physiological and phenomenological models. Physiological models aim at describing all the membrane currents that occur in cardiac cells (e.g. [4–6]). On the

other hand, phenomenological models aim at reproducing the integral characteristics of AP propagation in cardiac tissue (e.g. [2, 7]). In this work, we present a new efficient phenomenological model for ventricular epicardial cells with only three state variables. The proposed model is based on the Rogers-McCulloch formulation of the FitzHugh-Nagumo equations [8]. With respect to the Rogers-McCulloch formulation we added a new variable to describe the transient outward current and a shape factor to accurately fit the action potential morphology. Furthermore, we modified the definition of the timescale of the recovery variable to fit the experimental restitution properties. Our model allows to accurately reproduce the electrical activity of the epicardial tissue with only three state variables and is therefore more computationally efficient than existing models. Moreover, inspired by the work of Bernus et al. [9, 10], we included in the model a simplification parameter  $r_\gamma$ , whose effect is to scale down the excitation current during the upstroke. To maintain the same conduction velocity, we also multiplied the diffusivity by  $r_\gamma$ . Our approach allows increasing time and space integration steps by a factor equal to  $r_\gamma$ . The consequent reduction in computational time is similar to the theoretical value:  $r_\gamma^3$  in 2D and  $r_\gamma^2$  in 1D.

## 2. Methods

In our model the transmembrane current is represented as the sum of three contributions:

$$I_{ion} = gk(I_{exc} + I_{rec} + I_{to}) \quad (1)$$

where  $I_{exc}$ ,  $I_{rec}$ ,  $I_{to}$  are the excitatory, recovery, and transient outward currents, respectively. The definitions of excitatory and recovery currents is the same of the Rogers-McCulloch formulation:

$$I_{exc} = c_1 (V_M - B) \left( a - \frac{V_M - B}{A} \right) \left( 1 - \frac{V_M - B}{A} \right) \quad (2)$$

$$I_{rec} = c_2 u (V_M - B) \quad (3)$$

$r_\gamma$	1	1.5	2	3	4
$\alpha$	15	14	13.4	12.2	11.4

Table 1. Values of  $\alpha$  adopted for different simplification factors.

where  $V_M$  is the membrane potential and  $u$  is the recovery variable. The dynamics of  $u$  is defined by:

$$\frac{\partial u}{\partial t} = ke \left( \frac{V_M - B}{A} - u \right) \quad (4)$$

where  $e$  is the inverse of the time constant of the variable. We used a novel formulation for defining  $e$ :

$$e = \begin{cases} e_1 & \text{if } \frac{\partial u}{\partial t} \geq 0 \\ e_2 & \text{if } \frac{\partial u}{\partial t} < 0 \end{cases} \quad (5)$$

The shape factor  $g$  is formulated as follows:

$$g = \frac{(\gamma_0 + \gamma_1 u) (-\tanh(\alpha(u - \theta_u)) + 1)}{r_\gamma} + g_0 \quad (6)$$

where  $r_\gamma$  represents the simplification factor reducing the excitation current during the upstroke ( $r_\gamma > 1$ ). When changing the value of  $r_\gamma$ , the value of  $\alpha$  is adjusted so that the action potential duration (APD) in a single cell is unvaried (see Table 1). In order to maintain the same balance between excitatory and recovery current during upstroke, we defined  $e_1$  as follows:

$$e_1 = \begin{cases} ge_1^0 & \text{if upstroke} \\ e_1^0 & \text{otherwise} \end{cases} \quad (7)$$

The numerical implementation of this equation is trivial and will be discussed later. Finally, the transient outward current is defined through an additional variable  $w$ :

$$I_{to} = c_3 w (V_M - B) s_u \quad (8)$$

where  $s_u$  is defined as:

$$s_u = \frac{(u_M - u)^2}{u_M^2} \quad (9)$$

The third state variable  $w$  of our model is defined according the following differential equation:

$$\frac{\partial w}{\partial t} = ke_w \left( \frac{V_M - B}{A} - d_w w \right) \quad (10)$$

where  $d_w$  is formulated as follows:

$$d_w = \frac{d_w^0}{s_u} \quad (11)$$

Similarly to  $e_1$ , we defined  $e_w$  as:

$$e_w = \begin{cases} r_\gamma g e_w^0 & \text{if upstroke} \\ g e_w^0 & \text{otherwise} \end{cases} \quad (12)$$

We implemented 7 and 12 by identifying the upstroke as the interval when  $\frac{\partial V_M}{\partial t} \geq 0$  and  $\frac{\partial w}{\partial t} \geq 0$ . The parameter values adopted are shown in Table 2. They are optimized to reproduce experimentally measured properties of human epicardial tissue.

To simulate AP propagation, we incorporated our novel ionic current model in the monodomain formulation of cardiac tissue:

$$\frac{\partial V_M}{\partial t} - \nabla \cdot (r_\gamma D \nabla V_M) = -I_{ion} + I_{ext} \quad (13)$$

where  $I_{ext}$  indicates an external stimulation current. Note that the diffusivity is multiplied by the simplification factor  $r_\gamma$ . Therefore, when the ionic current is reduced in the upstroke, the conduction velocity remains unchanged. The diffusion coefficient  $D$  was set to  $1.171 \frac{cm^2}{s}$ , as in [2]. The proposed simplification allows increasing time and space integration steps by a factor equal to  $r_\gamma$ . Consequently, for the temporal integration we adopted the third order backward difference method with a time step of  $r_\gamma \cdot 0.1 s$ , whereas for the spatial integration we employed the finite element method with third order Lagrange elements and maximum element size equal to  $r_\gamma \cdot 0.75 mm$ . For two-dimensional simulations we used a triangular mesh.

One-dimensional simulations were performed on a  $2 cm$  long cable. The cable was stimulated at one end with a  $2 ms$  stimulus of strength twice the diastolic threshold. The restitution properties were computed through the steady-state restitution protocol [3]. Two-dimensional simulations were performed on a  $10 \times 10 cm$  square, which is large enough to prevent the boundaries from modifying the dynamic of the spiral waves. We employed the S1-S2 protocol [1, 4] to initiate spiral waves in the 2D sheet of ventricular epicardial tissue. The trajectory of the spiral tip was traced with the zero-normal-velocity method [11].

### 3. Results

Fig. 1 shows the action potential simulated in an isolated cell for different simplification factors. Our three-variable model accurately reproduces the AP morphology of epicardial cells. The value of  $r_\gamma$  does not significantly affect the AP morphology. The inset zooms on the AP upstroke and make possible to appreciate the slowdown of the upstroke dynamics for increasing values of  $r_\gamma$ .

Fig. 3 shows the APD and conduction velocity restitution curves reproduced by the proposed model for different values of  $r_\gamma$ , where  $r_\gamma = 1$  means no simplification.

$k$	$c_1$	$c_2$	$c_3$	$a$	$A$	$B$	$e_1^0$	$e_2$	$\gamma_0$	$\gamma_1$	$\theta_u$	$g_0$	$u_M$	$e_w^0$	$d_w^0$
$1000 \text{ s}^{-1}$	2.6	1	0.5	0.18	135 mV	-85 mV	0.0059	0.015	8	20	0.2	0.1	0.58	0.04	0.6

Table 2. Model parameters

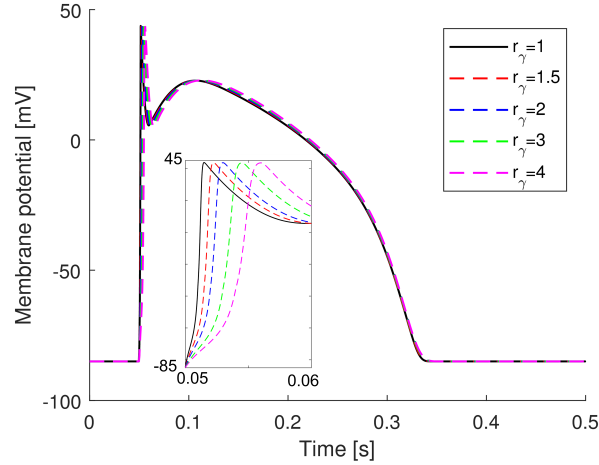


Figure 1. Action potential simulated with the proposed model for different values of  $r_\gamma$ . The inset zooms on the upstroke to better appreciate the upstroke velocity reduction due to the simplification.

The model shows a good agreement with the experimental data from [12] and [13]. Moreover, the simplification does not significantly alter the restitution properties. The maximum APD slightly grows when  $r_\gamma$  increases, presumably due to the stronger electrotonic coupling in the repolarization phase. The maximum conduction velocity also shows some slight variations (i.e. between  $69 \text{ cm/s}$  and  $71 \text{ cm/s}$ ) for different values of  $r_\gamma$ . Fig. 3 shows the reentry dynamics of the model for different values of  $r_\gamma$ . The dominant period experiences small variations between 262 and 279 ms, probably also due to the different meshes used for different values of  $r_\gamma$ . The values found agrees with experimental data from [15]. However, the simplification reduces the excitability of the model, altering the reentry dynamics. In particular, the trajectory of the spiral tip is substantially modified by the simplification. Without the simplification the spiral wave is characterized by a slightly meandering core where the tip trajectory for a single rotation traces an S-shaped core. Instead, when  $r_\gamma$  is increased the trajectory tends to a circle (as for  $r_\gamma = 3, 4$  in Fig. 3). The reduction in computational time introduced by the simplification is similar to the theoretical value:  $r_\gamma^3$  in 2D and  $r_\gamma^2$  in 1D.

#### 4. Conclusion

We developed a novel efficient phenomenological model for ventricular epicardial cells. Our model accurately re-

produces the main tissue-level characteristics of epicardial cells. Moreover, based on previous work by Bernus et al. [9, 10], we included a simplification parameter into the model. Note that, differently from [9, 10], our approach does not introduce any discontinuity in the ionic current which may lead to artefacts in the membrane potential. Due to the efficient computation, we believe the proposed approach could be useful in large-scale 3D simulations of heart electrical activity. Moreover, the simplification of our model can be tuned to the specific application by simply modifying  $r_\gamma$ . Finally, our formulation could also be extended to other types of cardiac cells.

#### References

- [1] Ten Tusscher KH, Panfilov AV. Alternans and spiral breakup in a human ventricular tissue model. *American Journal of Physiology Heart and Circulatory Physiology* 2006;291(3):H1088–H1100.
- [2] Bueno-Orovio A, Cherry EM, Fenton FH. Minimal model for human ventricular action potentials in tissue. *Journal of theoretical biology* 2008;253(3):544–560.
- [3] Elshrif MM, Cherry EM. A quantitative comparison of the behavior of human ventricular cardiac electrophysiology models in tissue. *PLoS one* 2014;9(1):e84401.
- [4] ten Tusscher KH, Noble D, Noble PJ, Panfilov AV. A model for human ventricular tissue. *American Journal of Physiology Heart and Circulatory Physiology* 2004;286(4):H1573–H1589.
- [5] Grandi E, Pasqualini FS, Bers DM. A novel computational model of the human ventricular action potential and ca transient. *Journal of molecular and cellular cardiology* 2010; 48(1):112–121.
- [6] O’Hara T, Virág L, Varró A, Rudy Y. Simulation of the undiseased human cardiac ventricular action potential: model formulation and experimental validation. *PLoS Comput Biol* 2011;7(5):e1002061.
- [7] Peñaranda A, Cantalapiedra IR, Bragard J, Echebarria B. Cardiac dynamics: a simplified model for action potential propagation. *Theoretical Biology and Medical Modelling* 2012;9(1):1–18.
- [8] Rogers JM, McCulloch AD. A collocation-galerkin finite element model of cardiac action potential propagation. *IEEE Transactions on Biomedical Engineering* 1994; 41(8):743–757.
- [9] Bernus O, Verschelde H, Panfilov AV. Modified ionic models of cardiac tissue for efficient large scale computations. *Physics in Medicine Biology* 2002;47(11):1947.
- [10] Bernus O, Verschelde H, Panfilov AV. Reentry in an anatomical model of the human ventricles. *International Journal of Bifurcation and Chaos* 2003;13(12):3693–3702.

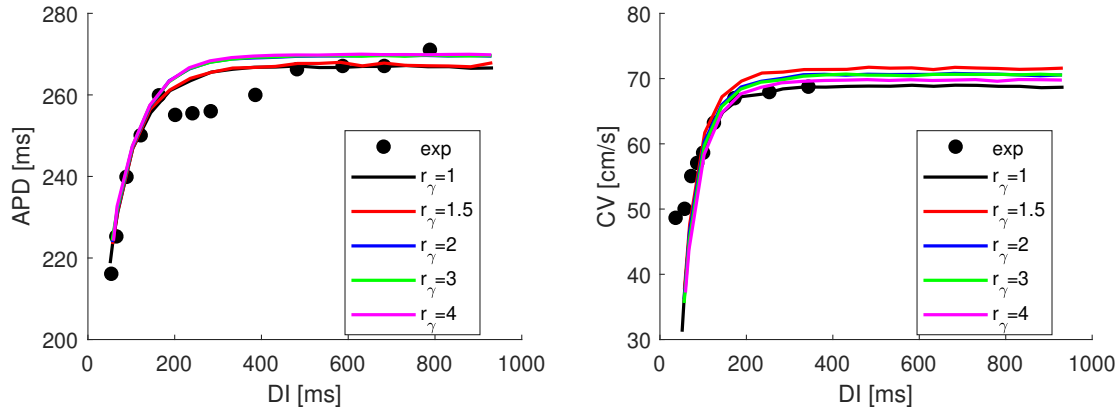


Figure 2. Restitution curves reproduced by the model for different values of  $r_\gamma$ . Experimental data from [12] and [13] are shown for comparison. As in [2, 4], the guinea pig data from [13] were rescaled by a factor of 0.92 to match the maximum CV of about 70 *cm/s* measured in human tissue [14].

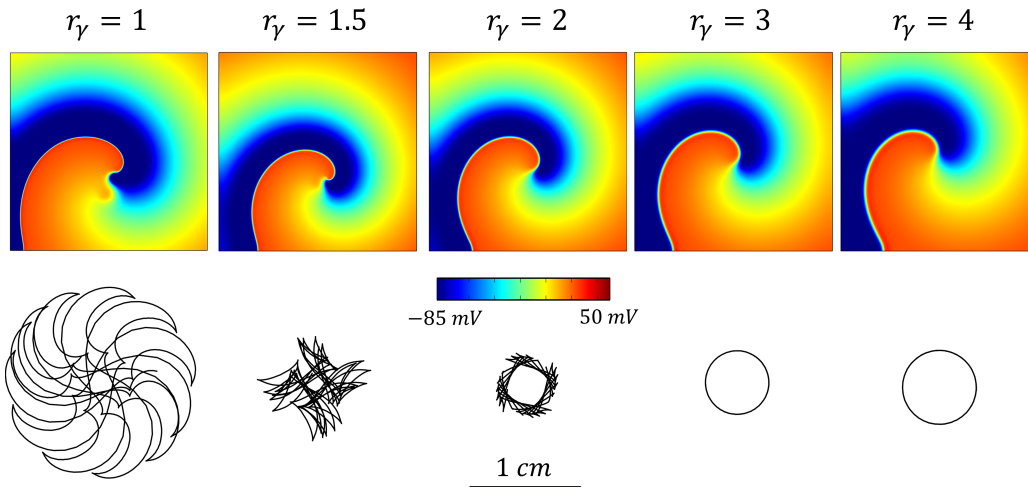


Figure 3. Reentry dynamics of the model for different values of  $r_\gamma$ . First row shows snapshots of the membrane potential during steady-state reentry. Second row shows spiral tip trajectories.

[11] Fenton F, Karma A. Vortex dynamics in three-dimensional continuous myocardium with fiber rotation: Filament instability and fibrillation. *Chaos An Interdisciplinary Journal of Nonlinear Science* 1998;8(1):20–47.

[12] Morgan JM, Cunningham D, Rowland E. Dispersion of monophasic action potential duration: demonstrable in humans after premature ventricular extrastimulation but not in steady state. *Journal of the American College of Cardiology* 1992;19(6):1244–1253.

[13] Girouard SD, Pastore JM, Laurita KR, Gregory KW, Rosenbaum DS. Optical mapping in a new guinea pig model of ventricular tachycardia reveals mechanisms for multiple wavelengths in a single reentrant circuit. *Circulation* 1996; 93(3):603–613.

[14] Taggart P, Sutton PM, Opthof T, Coronel R, Trimlett R,

Pugsley W, Kallis P. Inhomogeneous transmural conduction during early ischaemia in patients with coronary artery disease. *Journal of molecular and cellular cardiology* 2000; 32(4):621–630.

[15] Koller ML, Maier SK, Gelzer AR, Bauer WR, Meesmann M, Gilmour Jr RF. Altered dynamics of action potential restitution and alternans in humans with structural heart disease. *Circulation* 2005;112(11):1542–1548.

Address for correspondence:

Niccolò Biasi  
 Dip. Ing. dell'Informazione - Largo Lucio Lazzarino, 2, Pisa  
 niccolo.biasi@phd.unipi.it